JOURNAL OF CATALYSIS 53, 331–344 (1978)

The Transient Method Applied to the Methanation and Fischer–Tropsch Reactions over a Fused Iron Catalyst

HIROSHIGE MATSUMOTO[1] AND CARROLL O. BENNETT

Department of Chemical Engineering, University of Connecticut Storrs, Connecticut 06268

Received July 1, 1977; revised March 6, 1978

In the reduction of carbon monoxide with hydrogen to methane on a commercial iron catalyst, a transient method was used to study the reaction intermediates at 250°C and atmospheric pressure. When a stream of the reactant mixture (10% carbon monoxide in hydrogen) flowing over the catalyst in a steady state was suddenly changed to pure hydrogen, a surface intermediate was converted to methane at an initial rate higher than that at the steady state. The intermediate species was deactivated by a similar sudden change to helium. The reactivity of the reaction intermediate was much higher than that of carbon added to the catalyst by carburization by CO in argon. The results indicate that the surface of the active catalyst is covered mostly by a carbon intermediate, whose hydrogenation represents the rate-determining step. The bulk of the catalyst is Hägg carbide, Fe_2C.

INTRODUCTION

The steady-state flow method has been widely used in the kinetic study of Fischer–Tropsch and related syntheses. Careful measurements on many catalysts have been made by Vannice (*1*) and Dalla Betta *et al.* (*2*) by means of this method. The transient response method is very useful for the study of heterogeneous catalysis, and recent reviews describe the principle and applicability of this method (*3*, *4*).

We have used the transient method to study the reduction of carbon monoxide with hydrogen. One of the objectives of the present work is to get information is difficult to obtain by the conventional flow method. For example, when a stream of the reactant mixture (CO and H_2) flowing to the catalyst at steady state is suddenly changed to pure hydrogen or helium, the composition of the reaction products changes with time to reach a new steady state. Analysis of this phenomenon furnishes information concerning intermediate species on the catalyst at steady state.

The mechanisms for the catalytic synthesis of hydrocarbons from carbon monoxide and hydrogen have been the subject of much speculation and experiment because of the complexity of the reaction. The earliest theory of the reaction was the carbide theory (*5*, *6*). Metal carbonyls (*7*) and methylene radicals (*8*) were also proposed as the reaction intermediates. Recently, Wise and co-workers (*9*) and Araki and Ponec (*10*) suggested a surface carbon species as an intermediate for methanation on a nickel catalyst. Another well-known idea is that an adsorbed complex of formula HCOH is formed during hydrocarbon synthesis. This theory was

---

[1] Department of Chemistry, University of Nagasaki, Japan.

0021-9517/78/0533-0331$02.00/0

proposed by Storch, Golumbic, and Anderson (*11*) and modified by Kummer and Emmett (*12*) and by Hall *et al.* (*13*).

EXPERIMENTAL

The transient experiments were performed at 250°C under atmospheric pressure. The gases were switched by means of a four-way valve. The flow system was carefully designed so that this switch did not alter the pressure in the reactor or the flow rate measured by a soap-bubble flowmeter. The analysis of the reactants and products was carried out by a mass spectrometer (residual gas analyzer 21-614, Consolidated Electrodynamics). The mass spectrometer was suitably calibrated by known pure gases and gas mixtures for each run to allow for the cracking patterns. The continuous inlet system to the mass spectrometer has a response time sufficiently small (~12 sec) to permit good resolution of an inlet step function. The tubular reactor made from stainless steel was held in an electronically controlled furnace of large heat capacity to keep the temperature constant. The maximum variation of temperature over the reactor was less than 1°C. Fifty milligrams of the catalyst was held between silica beads to minimize the dead volume of the reactor. It was established that the silica beads and the stainless steel reactor were inactive for the reaction.

The iron catalyst used in the present work was CCI fused magnetite catalyst with the following composition: Fe_3O_4, 96.5%; Al_2O_3, 2.5%; K_2O, 0.6%; and SiO_2, 0.4%. The catalyst was reduced in a hydrogen stream at about 60,000 per hour for a period of 48 hr at 450°C before use. The surface area of the reduced catalyst was determined to be 13.0 m^2/g by the BET method, equivalent to about 135 μmole/g of Fe_3O_4. The particle size of the catalyst used ranged from 250 to 300 μm. The reaction mixture was 10.02% carbon monoxide in hydrogen. The gases used in this experiment have no peak of mass number 32 in the mass spectrum. The iron surface of the reduced catalyst adsorbed 38 μmole of CO/g of Fe_3O_4 at −78°C, so that about 72% of the surface is covered by promoters (*14*). The classical volumetric method was used; following Solbakken *et al.*, one CO molecule per active site is assumed.

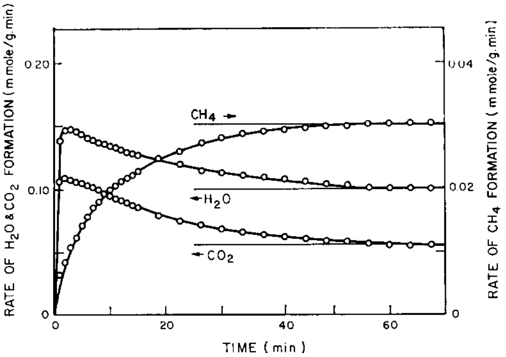

FIG. 1. Formation of major components as a function of exposure time.

RESULTS

The freshly reduced catalyst took approximately 60 min to attain a steady state for the formation of methane, water, and carbon dioxide. After the catalyst was reduced with hydrogen for 48 hr at 450°C, the system was cooled down to the reaction temperature, 250°C, in a hydrogen stream. Prior to exposure to the carbon monoxide–hydrogen mixture, the catalyst was treated with helium for 1 hr at 250°C to remove the adsorbed hydrogen. On the introduction of the reaction mixture to the pretreated catalyst at a flow rate of 390 cm^3/min/g, immediate formation of water and carbon dioxide as observed in the outlet gas, as shown in Fig. 1. These formation rates decreased slowly with the time on-stream and reach steady-state values after 1 hr. On the other hand, the methane formation rate increased gradually with time and also reached a steady state after 1 hr. The

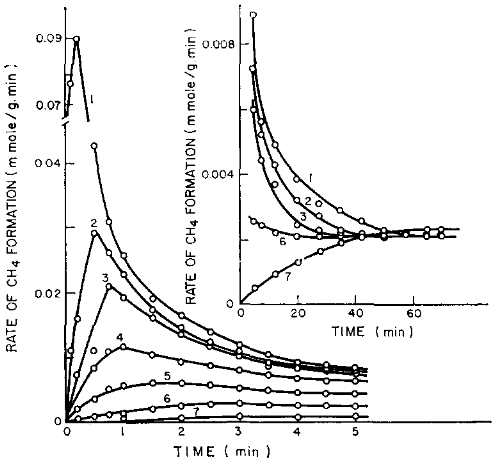

FIG. 2. Methane formation by hydrogen flushing of the steady-state catalyst after helium treatments of various lengths of time: (1) 0 min; (2) 1 min; (3) 5 min; (4) 30 min; (5) 90 min; (6) 270 min; (7) 1080 min.

periods required to get to steady values depended on the composition of the reactant and on the reaction temperature. At steady state at 250°C, the yield of methane is about 1.8% of the CO feed.

The computation of reaction rates from observed transient data is much simplified by the low conversions used in the differential reactor. The corresponding high gas velocity through the bed and the small particle size ensure that there are no transport limitations. For a differential reactor, the mass balance for a component j not present in the feed is

$$\frac{d\bar{C}_j}{dt} = \bar{r} - \frac{C_j}{\theta}, \tag{1}$$

where

θ = residence time V/q (min)
V = void volume of reactor
q = flow rate (ml/min)
C_j = outlet concentration of j (mole/ml)
$\bar{C}_j$ = average C_j in the reactor (mole/ml)
$\bar{r}$ = reaction rate (mole/min/ml)

For all data reported here, $\theta = 4 \times 10^{-4}$ min. The C_j value for methane is typically 7.5×10^{-8} mole/ml, and $d\bar{C}_j/dt$ is never more than 10^{-7} mole/min/ml. Thus, the derivative is negligible, and it is sufficiently accurate to report rates calculated by the equation:

$$\bar{r} = C_j/\theta \tag{2}$$

or

$$r = C_j q/W \tag{3}$$

in mmole/min/g, where W is grams of magnetite.

When the stream of the reaction mixture flowing to the catalyst in the steady state was suddenly changed to pure hydrogen at the same flow rate, immediate formation of a large amount of methane was observed. The methane formation rate then rapidly decreased with the time on stream of hydrogen, and then reached a pseudo-constant value of 0.002 mmole/g min with 1 hr, as shown in Fig. 2. During the course of the hydrogen flushing, the only major component other than methane was water, although small amounts of higher hydrocarbons, such as ethane and propane, were observed at the beginning of the flushing.

During the transient experiments the only hydrocarbon followed was methane (m/e = 15); higher hydrocarbons were observed qualitatively by peaks at 29 and 43. The steady-state distribution of hydrocarbons corresponding to a flow of 390 ml/g/min of the 10 mole% CO in H_2 over 50 mg (unreduced) of catalyst at 250°C and 1 atm was also measured by gas chromatography (*16*). A Porapak Q column was used at 180°C with a flame ionization detector. The results are expressed as mole ratios to methane: $C_2/C_1 = 0.39$; $C_3/C_1 = 0.32$; $C_4/C_1 = 0.15$; and $C_5/C_1 = 0.06$. Samples taken at 5, 30, and 60 min after a switch from H_2 to the feed mixture (Fig. 1) give these same ratios, to within about 5%.

The steady-state rate, 29 μmole of CH_4/g/min, can be expressed as a turnover frequency by dividing by the CO adsorption, 38 μmole/g. The result is 12.7×10^{-3} s^{-1}, assuming one CO adsorbed per site on iron (*15*). Converted to the conditions of Vannice (*1*), the rate is 26.9×10^{-3} s^{-1} at 25% CO in H_2 and 275°C. Vannice, however, assumed bridged CO bonding, and this gave a rate of 57×10^{-3} s^{-1}. The difference is at least partly a result of the differing catalysts. Vannice used 15% Fe on Al_2O_3; in this work the catalyst is iron promoted with K_2O and Al_2O_3. The activities differ less on the basis of CO reacted: 160×10^{-3} s^{-1} (Vannice) vs 96×10^{-3} s^{-1} (this work).

The higher hydrocarbons produced with methane explain the presence of so much water and CO_2 in the product (Fig. 1). Although CO_2 is the principal by-product at high conversion, at the low conversion reported here, H_2O is more abundant. All the water and carbon dioxide observed cannot be accounted for by the hydrocarbons up to pentane that were observed. Small amounts of higher hydrocarbons are probably undetected, and of course the production of one C_nH_{2n+2} involves the production of n molecules of water or carbon dioxide. No olefins were observed.

When the catalyst in the steady state was exposed to a pure helium stream, neither methane nor carbon dioxide was observed, but an appreciable amount of water was detected in the outlet helium stream. After a certain period of the helium flushing, the feed to the reactor was switched to hydrogen. An appreciable amount of methane was formed on this introduction of hydrogen; small quantities of ethane and propane were also observed. The results are shown in Fig. 2 for various periods of helium treatment. The formation rate of methane was found first to increase and then to decrease with time on-stream for hydrogen. The time for the maximum methane formation rate increased with increasing period of helium treatment. The catalyst treated by helium overnight showed no such point. For all the catalysts, with various treatments, the same pseudo-steady formation rate of methane as that after 1 hr of hydrogen flushing was observed. This methane formation rate was 0.002 mmole/g/min and was constant for many hours; naturally, it must eventually fall to zero. After a 1-hr treatment by hydrogen, the temperature was elevated from 250 to 450°C at a rate of about 10°C/min in the hydrogen. The rate of methane formation strongly increased with the temperature, and the maximum formation rate was observed at approximately 400°C. The total amount of methane formation by hydrogen flushing at both temperatures was estimated to be 5.7 mmole/g, which was independent of the period of the helium treatment, within experimental error. It might be considered that at least two kinds of compounds are associated with the catalyst in the steady state. One type is reduced to methane by hydrogen with an appreciable rate at 250°C. This type of species is deactivated on the surface by helium flushing, since no appreciable amount of carbonaceous compound was observed in the gas phase during the helium treatment. The other type is slowly converted to methane by hydrogen. This type of species is not completely removed or deactivated, even by overnight helium treatment, although it is rapidly removed by hydrogen as the temperature is programmed to 450°C.

If it can be postulated that the former species acts as the reaction intermediate determining the actual rate of methane formation at steady state, the rate of hydrogenation of the intermediate can be determined from the results shown in Fig. 2, assuming a first-order dependence of the rate on the amount of intermediate. For surface species X reacting to methane, Eq. (1) becomes

$$\frac{d[\mathrm{X}]}{dt} = r, \qquad (4)$$

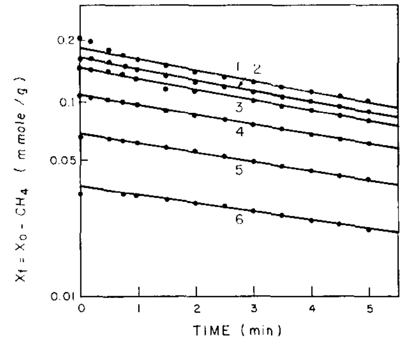

FIG. 3. First-order dependence of methane formation from the intermediate on the steady-state catalyst after helium treatments of various lengths of time: (1) 1 min; (2) 5 min; (3) 30 min; (4) 90 min; (5) 270 min; (6) 1080 min.

and Eq. (3) holds for methane, written as

$$r = \frac{q}{W}[\mathrm{CH_4}], \tag{5}$$

where [X] and $[\mathrm{CH_4}]$ are the amount of the intermediate on the surface and that of methane formed from the intermediate, respectively. Thus $d[\mathrm{X}]/dt$ is measured by the rate of methane formation, as is shown in Fig. 2. The accumulated methane formed is $[\mathrm{CH_4}]_t$, found from $\int_0^t r dt$, the area under a curve in Fig. 2. Thus the amount of intermediate is given by:

$$[\mathrm{X}]_t = [\mathrm{X}]_0 - [\mathrm{CH_4}]_t. \tag{6}$$

If surface hydrogen is kept at a high concentration by the hydrogen flushing, the rate of hydrogenation of X should be first order in X after the initial increase of methane appearance rate shown in Fig. 2:

$$\frac{-d[\mathrm{X}]}{dt} = k[\mathrm{X}]. \tag{7}$$

Integration yields

$$\ln [\mathrm{X}]_0 - \ln [\mathrm{X}]_t = kt \tag{8}$$

and

$$\ln \{[\mathrm{X}]_0 - [\mathrm{CH_4}]_t\} = \ln [\mathrm{X}]_0 - kt, \tag{9}$$

where $[\mathrm{X}]_0$ and $[\mathrm{X}]_t$ represent the amount of the intermediate on the surface before hydrogen flushing and after t minutes in hydrogen, respectively. According to the previous discussion, $[\mathrm{X}]_0$ for each catalyst can be determined by subtracting the total amount of methane formed within 1 hr at 250°C for the catalyst treated overnight by helium from the amount formed for each catalyst with the various helium treatments. Furthermore, $[\mathrm{CH_4}]_t$ can also be estimated from the difference in the amount of methane formed over the catalyst with various helium treatments and that formed over the catalyst with overnight helium treatment. The logarithms of $\{[\mathrm{X}]_0 - [\mathrm{CH_4}]_t\}$ are plotted against the time in Fig. 3 according to Eq. (9). The data show good linear relationships and have practically the same slopes.

An appreciable amount of water was detected simultaneously on the introduction of helium to the catalyst in the steady state, although neither methane nor carbon dioxide was observed during this period. The amount of water formation during the helium flushing is shown in Fig. 4, along with that during the hydrogen flushing. On the introduction of helium to the catalyst in the steady state at 250°C, the peak corresponding to mass number 18 decreased rapidly at first and

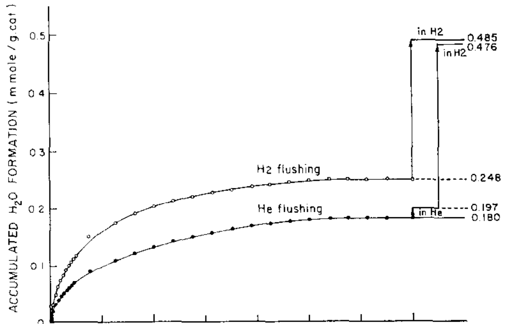

FIG. 4. Amount of water removed from the steady-state catalyst by helium and hydrogen flushing.

TABLE 1

Influence of Helium Treatment on Surface Intermediate

He treatment (min)	CH_4 formed within 65 min (mmole/g)	X on the surface (mmole/g)	X deactivated by He (mmole/g)	H_2O removed by He (mmole/g)	k for CH_4 from X (min^{-1})
0	0.31	0.20	0	0	0.12
1	0.26	0.15	0.05	0.03	0.12
5	0.25	0.14	0.06	0.07	0.12
30	0.19	0.08	0.12	0.15	0.12
90	0.16	0.05	0.15	—	0.11
270	0.14	0.03	0.17	—	0.11
1080	0.11	0	0.20	0.20	—

then slowly. After 70 min, the water formation almost ceased. The amount of water formed in this stage was estimated to be 0.18 mmole/g. At this point, the temperature was elevated in the helium to 450°C, where only 0.017 mmole/g of water was formed. When the stream of helium flowing to the reactor was changed to hydrogen at 450°C, formation of water (0.29 mmole/g) occurred at an appreciable rate. If hydrogen flushing was carried out in a manner similar to the helium flushing, 0.248 and 0.237 mmole/g of water were formed at 250 and 450°C, respectively. There is no appreciable difference in the total water formation between the first run (0.476 mmole/g) and the second run (0.485 mmole/g). The difference in the water formation at 250°C between flushing by helium and by hydrogen is presumably due to the removal of surface oxygen and hydroxyl groups by hydrogen, plus probably some bulk oxygen.

The results calculated from the data in Figs. 2, 3, and 4 are summarized in Table 1. The amount of methane formed by hydrogen flushing at 250°C decreased with the period of helium flushing. The calculated amount of the intermediate species which was deactivated by the helium treatment increased with the period of the treatment. Furthermore, the rate constant for methane formation from the intermediate species, calculated from the slopes of the plots in Fig. 3, was substantially independent of the helium treatment and was estimated to be 0.12 min^{-1}.

The steady-state catalyst was studied by X-ray diffraction, and only the peaks corresponding to Hägg carbide, Fe_2C, were observed. The sum of the amount of carbon removed as methane by H_2 at 250°C and that removed as the temperature is increased to 450°C is 5700 μmoles/g, for 12,540 μmoles of iron per gram. The corresponding stoichiometry is $Fe_{2.2}C$. Although the bulk of the catalyst is carbided at steady state, its active surface is probably in a reduced state. At high conversion and at higher CO/H_2 ratios, the bulk of the catalyst is known to be partly oxidized (*17*). The reduced catalyst, before exposure to CO/H_2, but passivated in CO_2, showed only the peaks of α-iron.

The experiments described so far concern the initial transient period when the reduced catalyst is first exposed to CO/H_2, the steady state, and the effect of switching the feed at steady state to H_2 or to He for various times followed by H_2. We now consider the transients obtained if the CO/H_2 feed is redirected over the catalyst after these various treatments by hydrogen or helium.

Figure 5 shows the responses obtained at 250°C when the steady-state catalyst

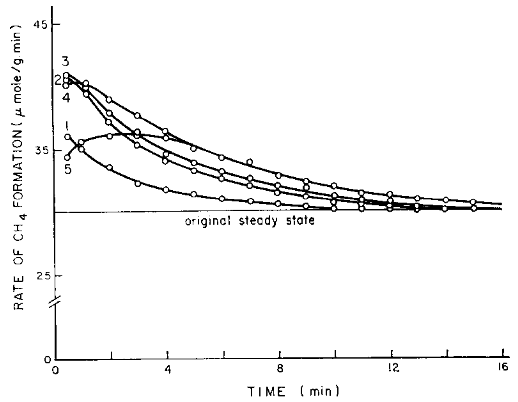

FIG. 5. Methane formation after various hydrogen treatments of the catalyst in the steady state: (1) 1 min; (2) 5 min; (3) 10 min; (4) 30 min; (5) 60 min.

is treated by hydrogen for various times and then treated by the CO/H_2 feed mixture. Zero time on the graph corresponds to the switch to the CO/H_2 mixture. The initial points for these curves would be points at the appropriate times taken from curve 1 of Fig. 2. There is an immediate jump in the methane formation rate (or concentration) on reintroduction of CO to the H_2 stream. The overshoot increases with time of H_2 exposure and then begins to fall as the catalyst bulk begins to be decarburized. A long treatment in H_2 at 450°C would of course bring the system back to the initial point of Fig. 1.

The effects of various exposures of the steady-state catalyst to helium are shown in Fig. 6. Instead of a switch to hydrogen after these exposures to helium, as is shown in the various curves of Fig. 2, we switched to the 10.2% CO/H_2 mixture after various exposures to helium. A very short exposure to helium leaves the catalyst essentially unchanged, and the steady state is almost immediately reestablished. Longer treatments by helium, however, lead to a slower increase in methane production and to a reduction of the eventual steady-state activity. A reduction by hydrogen at 450°C, however, returns the catalyst to its state at the beginning of Fig. 1.

A comparison of Figs. 2 and 6 shows that the fraction of intermediate removed or inactivated, as measured by hydrogen flushing after the helium treatment, is much larger than the fractional reduction of the steady-state activity after the similar helium exposures shown in Fig. 6. Recall that no methane or CO_2 is desorbed during helium treatment at 250°C.

The effect of CO alone on the reduced catalyst has also been studied. A typical result of the interaction of carbon monoxide with the fused iron catalyst is shown in Fig. 7. The system was flushed with helium for 1 hr at 250°C after hydrogen reduction at 450°C. When the flow is changed to 10% carbon monoxide in argon, after a short initial period, constant concentrations of carbon monoxide and carbon dioxide were observed in the outlet gas stream during the first 100 min. After this period, the rates of carbon monoxide consumption and carbon dioxide formation decreased with time on-stream. During the course of the reaction, the ratio of carbon monoxide consumed to carbon dioxide formed remained constant at about 2. No appreciable amount of oxygen

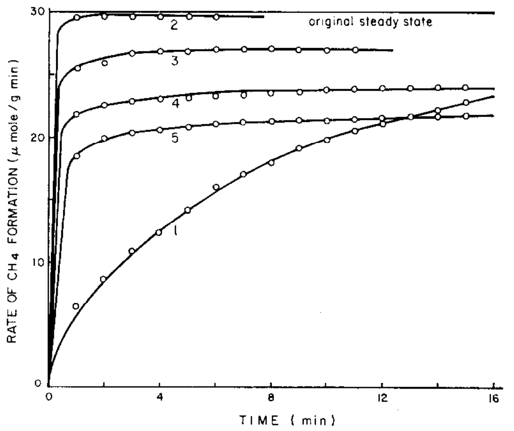

FIG. 6. Methane formation after various helium treatments of the catalyst in the steady-state: (1) freshly reduced catalyst; (2) 1 min; (3) 5 min; (4) 30 min; (5) 60 min.

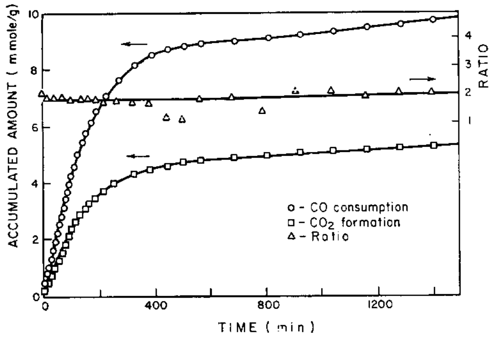

FIG. 7. Amounts of CO consumption and CO_2 formation during the course of CO decomposition. Concentration of CO in feed, 9.9%; temperature, 250°C; flow rate, 212 cm^3/min/g.

in the gas phase was observed in this reaction. Essentially, the same result was obtained if carbon monoxide was introduced immediately after hydrogen reduction without helium treatment. By X-ray examination of the catalyst, diffraction patterns of α-iron and Hägg carbide, with composition approximating Fe_2C, were observed in the early stage of the reaction. With an increase in time on-stream, the height of the diffraction pattern for the former decreased, whereas that for the latter increased. The catalyst showed only the diffraction pattern of Hägg carbide after 1000 min of treatment by carbon monoxide. No crystalline carbon material, such as graphite, was found, even after 1500 min. Therefore, the main reaction of carbon monoxide decomposition on the fused iron catalyst is

$$2CO + 2Fe \rightarrow Fe_2C + CO_2. \qquad (10)$$

The amount of carbide could be estimated from the carbon dioxide formation. At higher temperatures, above 400°C, the main product in the reaction between iron and carbon monoxide is cementite, Fe_3C (*18*). Anderson *et al.* (*17*), however, confirmed the exclusive formation of the Hägg carbide during the Fischer–Tropsch synthesis on a similar fused iron catalyst at temperatures comparable to those of the present work.

Bousquet *et al.* (*19*) and Tøttrup (*18*) reported that a constant rate of weight increase was observed after an initial rapid weight increase in thermogravimetric studies of the nickel–carbon monoxide system. They assumed that the initial weight increase was caused by adsorption of carbon monoxide on the nickel surface. In order to understand the initial stage of the carbon monoxide–iron interaction, 2% carbon monoxide in argon was used as feed. The result is shown in Fig. 8, where the amount of carbon is estimated from the carbon monoxide consumption. Neither carbon monoxide nor carbon dioxide was observed in the outlet gas stream for about 45 s, and then a constant consumption of carbon monoxide and a constant formation of carbon dioxide were observed after about 20 min. The absence of reactant and product in the gas phase during the initial stage is presumably due to adsorption of carbon monoxide on the surface, which corresponds to the initial rapid weight increase in the thermogravimetric experi-

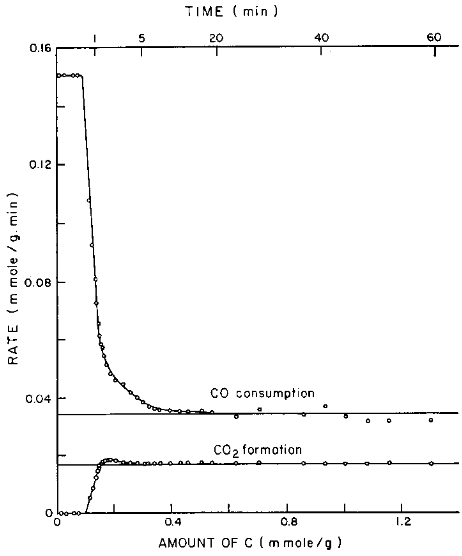

FIG. 8. Rates of CO consumption and CO_2 formation during the course of CO decomposition. Concentration of CO in feed, 2.0%; temperature, 250°C; flow rate, 230 cm^3/min/g.

TABLE 2

Catalyst Carburization by CO in Ar[a] and Its Methanation by H_2 Flushing (mmole/g)

CO treatment (min)	Total C[b]	C with CO_2 formation[c]	C without CO_2 formation	CH_4 formed by H_2[d]
5	0.25	0.07	0.18	0.16
10	0.36	0.16	0.20	0.27
20	0.54	0.33	0.21	0.42
40	0.88	0.68	0.21	0.87
70	1.39	1.20	0.19	1.43

[a] 2% CO in Ar.

[b] Calculated from CO consumption.

[c] Calculated from CO_2 formation.

[d] Total methane formed at 250 and 450°C.

ments (*18*, *19*). When the stream of carbon monoxide–argon mixture flowing over the catalyst was suddenly changed to pure helium, neither carbon monoxide nor carbon dioxide was detected in the helium stream. Thus, the adsorption of carbon monoxide was irreversible. The initial period shown in Fig. 8 is too short to be visible in Fig. 7; also, in the latter figure it is shortened by the higher CO concentration (10% vs 2%). The amounts of carbon associated with the catalyst when treated by carbon monoxide for various periods are cited in Table 2. The amount of carbon associated with carbon dioxide formation was essentially proportional to the period of carbon monoxide treatment, whereas that without carbon dioxide formation was independent of the time on-stream.

It is clear that the carbon associated with the catalyst is mostly in the form of the bulk carbide Fe_2C. The changes during treatment by 10% CO in Ar are characterized, however, in terms of "amount of carbon." At the end of about 1600 min, the iron is almost completely carbided by CO. Figure 1 shows, however, that only about 60 min is required to carburize the catalyst by a mixture of 10% CO in hydrogen. We shall see presently that the catalyst carburized by CO/Ar becomes inactive for methanation, whereas that treated by CO/H_2 achieves the steady-state activity shown in Fig. 1.

Wise and co-workers reported (*9*) that, in a carbon monoxide–nickel system, the surface carbon can be rapidly and quantitatively converted to methane by hydrogen at 280°C. In order to measure the reactivity of carbon species associated with the iron catalyst, pure hydrogen was passed over the catalyst carburized by carbon monoxide which was diluted with argon at 250°C. The result is cited in the last column of Table 2. On exposure of the carburized catalyst to hydrogen, methane slowly formed. No higher hydrocarbons were observed in the outlet gas. Only 50 to 70% of the carbon calculated from carbon monoxide consumption, however, was converted to methane at 250°C during a 300-min exposure to hydrogen. After this period, the temperature was elevated to 450°C at a rate of 10°C/min in hydrogen. The maximum methane formation was observed approximately at 400°C for catalysts with various extents of carburization. It may be assumed that the total amount of methane formed by hydrogen flushing corresponds to the amount of carbon combined with the catalyst.

To check the reactivity of the carbon combined with the fused iron catalyst, the rate of hydrogenation was measured for the catalyst with various amounts of carbon incorporated. The results are shown in Fig. 9. In this experiment, the carburized catalyst was prepared by the disproportionation of carbon monoxide, and hydrogenation was carried out by switching to hydrogen feed, just as was done for the steady-state catalyst already described. The initial rates of hydrogenation for various amounts of carbon were obtained from the initial slopes of the curves in Fig. 9. These initial rates are plotted against the amount of combined carbon in Fig. 10. In this figure, the rates of methane formed from the intermediate X,

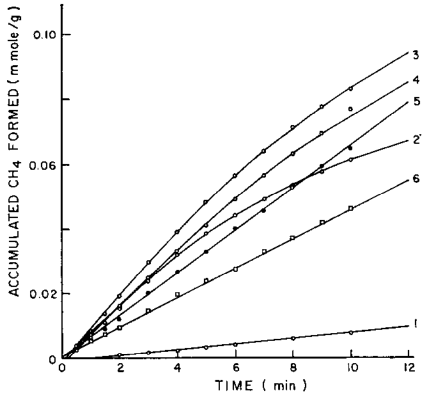

FIG. 9. Amount of methane formed by hydrogen flushing the catalyst incorporating various amounts of carbon at 250°C: (1) 0.13 mmole of C/g; (2) 0.25 mmole of C/g; (3) 0.36 mmole of C/g; (4) 0.54 mmole of c/g; (5) 0.88 mmole of c/g; (6) 1.39 mmole of c/g.

as calculated from the results in Fig. 2, are also plotted against the amount of X for comparison. The rate of methane formation from the combined carbon first increased with increasing amount of combined carbon, and a maximum rate of 0.01 mmole/g min was observed at 0.4 mmole/g. A further increase in the amount of carbon resulted in a decrease in the initial rate of hydrogenation to methane. This decrease is presumably caused by a decrease in surface sites available for hydrogen adsorption. On the other hand, the rate of methane formation from the intermediate complex X increased proportionally with increasing amount of X. The striking difference in the rate of hydrogenation between the intermediate complex and the carbon formed by CO suggests that the effective reaction intermediate on the fused iron catalyst is not the same as this carbon introduced into the catalyst by CO.

The hydrogenation of the carbon formed by the disproportionation of carbon monoxide gave methane as the only hydrocarbon product, whereas the similar hydrogenation of X gave definite quantities of ethane and propane. Whatever role the

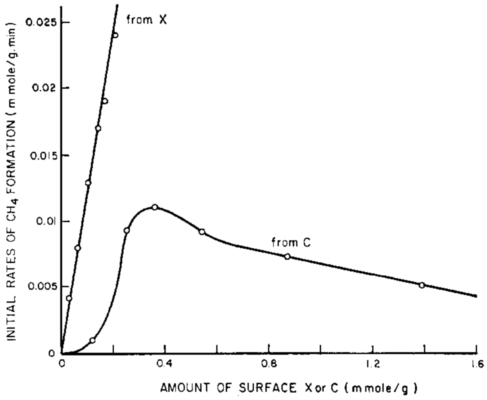

FIG. 10. Initial rates of methane formation by hydrogen flushing from the intermediate X and from carbon formed by exposure to CO alone.

combined carbon may play in methane production, it is probably not active in chain building on the surface of the iron catalyst.

The catalysts containing various amounts of carbon incorporated by treatment at 250°C by CO/Ar for various times were also used for the methanation reaction. At the end of the exposure to 10% CO in argon, the feed was switched to 10% CO in hydrogen. The results for the methane response are shown in Fig. 11. This graph recalls to some extent the behavior of the helium-treated catalysts (Fig. 6). A relatively short initial transient is observed. This period decreased with increasing amount of carburization, up to 1.9 mmole/g. The catalyst con-

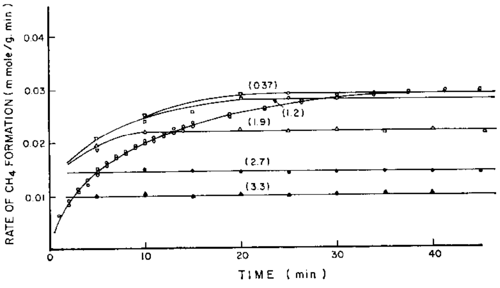

FIG. 11. CH_4 formation on the catalyst covered with various amounts of carbon. Numbers on the curves represent amounts of carbon in mmole/g.

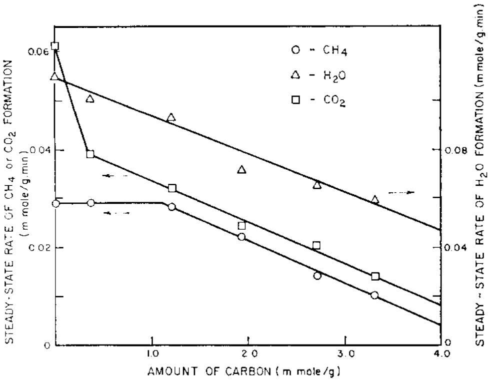

FIG. 12. Relation between the steady-state rate and the amount of carbon introduced by CO/Ar.

taining 2.7 and 3.3 mmole/g of carbon showed no substantial initial transient period. On the other hand, in the formation of water and of carbon dioxide, no such initial period was observed for either the fresh or the carburized catalyst. At the initial stage of the reaction, the rate of water formation on 1.2 and 1.9 mmole/g carburized catalyst was higher than that on the fresh catalyst, whereas the rate of carbon dioxide formation decreased monotonically with the amount of carbon.

The steady-state rates of product formation plotted against the amount of carbon are shown in Fig. 12. The steady-state rates of water and carbon dioxide formation decreased with increasing amount of carbon. On the other hand, the steady-state rate of methane formation was essentially independent of carbon up to 1.2 mmole/g and then decreased with increasing carbon.

DISCUSSION

The iron catalyst is slowly carburized by CO, as shown in Fig. 7. Some "surface carbon" may form at the same time, but it could not be identified experimentally. At any rate, the carbon formed by CO is much less reactive with hydrogen for the formation of CH_4 than the carbon-containing intermediate X, as shown in Fig. 10. Also, the intermediate gives higher hydrocarbons, whereas the carbide from CO does not. Thus, it appears that the intermediate is not the Hägg carbide, but may be some kind of active carbon or, of course, adsorbed CO, CHOH, CH_2, or others.

Figure 1 shows that the carburization of the catalyst is much more rapid in CO/H_2 than is CO/Ar. The hydrogen reacts with the oxygen left on the surface or in the bulk by the decomposition of CO, so that more of the surface is available for the intermediate leading to Fe_2C. From the initial ratio of H_2O/CO_2 observed, the overall reaction is approximately

$$4CO + 6Fe + 2H_2 \rightarrow 2H_2O + CO_2 + 3Fe_2C. \quad (11)$$

This process is occurring in Fig. 1. It is important to notice that the rate of methane production increases from an initial value of zero. This result implies that the rate-determining active center is increasing in concentration as the iron is carburized. Its reactivity towards carburization of the bulk of the iron must be high, so that its concentration is proportional to the extent of carburization. In other words, the intermediate X formed from CO and H_2 is the intermediate for the formation of both Fe_2C and CH_4. If carburization plus deposition of surface carbon were poisoning the catalyst, the rate of methane formation should decrease from a maximum at time zero.

When the flow of H_2/CO at steady state is abruptly changed to H_2 alone, the rate of methane formation quickly jumps to a much higher value (Fig. 2). At steady state, the surface is largely covered with X, but adsorbed hydrogen must be necessary for the reaction. When the CO is cut off, the surface hydrogen rapidly increases, as does the rate of CH_4 production. The surface hydrogen concentration, however, can increase severalfold for a very small reduction in the coverage by X. Hydrogen then is present effectively in excess, and the X decays in a first-order manner, as illustrated by Fig. 3. It is clear that, at steady state, the rate is determined by the hydrogen concentration only, in accord with the well-known rate law for the Fischer–Tropsch reaction, $r = k\ (H_2)$ at low conversion (*20*).

As the X is removed by hydrogen, the rate of methane formation eventually falls to a pseudo-steady value, probably corresponding to the rate decarburization of Fe_2C by H_2 at 250°C. As the temperature is programmed to 450°C, the H_2 quickly reduces the catalyst to α-iron once more.

Since X seems to be the rate-limiting intermediate for both carburization and methanation, it seems more probable that it is *–CO or *–C rather than *CHOH.

Figure 5 shows that short treatments of the steady-state catalyst result in an overshoot in methane production upon return to a CO/H_2 feed. The hydrogen has removed X and oxygen from the surface, the latter as water, as shown in Fig. 4. After this treatment, the catalyst is temporarily more active than at steady state. The bulk Fe_2C has an active surface of relatively clean Fe. Figure 5 also shows that longer treatments in H_2 eventually lead to a smaller overshoot as some bulk decarburization occurs. If the catalyst is sufficiently decarburized, the rate, i.e., the concentration of X, will be reduced until the iron is recarburized. A sufficiently drastic exposure to H_2, of course, returns the catalyst to time zero of Fig. 1.

The treatments with helium illustrated by Figs. 2 and 4 were intended to detect desorption from the steady-state catalyst; only water was observed to desorb. The unexpected result, however, was the subsequent deactivation of the active species X. As already described, about 200 μmole/g of X is deactivated by a sufficiently long exposure to He. Since an equivalent amount of water is desorbed (Table 1, Fig. 4), it is tempting to associate the helium treatment with the decomposition of CHOH. Most of the water, however, may be desorbed from the surface of the promoters.

Alternatively, exposure to He may cause surface carbon to rearrange to a form which is relatively inactive at 250°C. Since X is also the precursor of Fe_2C, however, in the absence of H_2 and CO, it may combine with bulk iron and become inactive to H_2. Figure 6 shows that reexposure to H_2/CO feed results in an eventual steady-state rate that is only reduced by one-third after the deactivation of all the X. Thus, part of the X forms a carbide or carbon inactive in H_2/CO or H_2 at 250°C, and the rest forms a carbide or carbon inactive in H_2 but which does not prevent reaction in H_2/CO at 250°C. As usual, H_2 at 450°C returns the catalyst to its original state.

Figures 11 and 12 show that a given degree of carburization produced by CO/Ar gives a catalyst which is quite different from one produced from CO/H_2. For the former, after a certain degree of bulk carburization it must be assumed that the surface is also gradually poisoned by combined carbon, as has been observed by Podgurski *et al.* (*21*). In the presence of hydrogen adsorbed on the surface, the bulk carburization occurs with little effect on the surface, which remains largely iron covered by adsorbed species (*–X, *–O, etc.) and remains active for methanation and the Fischer–Tropsch reaction.

In the preceding discussion, the major observed phenomena have been explained in terms of a rate-determining active center X; the rate determining step is the reaction of X with adsorbed hydrogen to give further steps in the sequence leading to hydrocarbons. Since about 200 μmole/g of X exist at steady state and CO adsorption at −78°C is only 38 μmole/g, it is evident that the area per C atom of X must be only about one-fifth that of CO, to be consistent. This might lead to the postulation of surface carbon as the identity of X. This conclusion would also be consistent with the well-verified tendency of iron to absorb CO disassociatively, especially at 250°C. The rate-determining step would then be the hydrogenation of *–C, which covers most of the surface.

For chain growth to hydrocarbons other than methane, there is some evidence that adsorbed CO may be necessary (*22*). It could add to $*\text{–}CH_3$ to form $*\text{–}\underset{\underset{\displaystyle O}{\|}}{C}\text{–}CH_3$, leading to oxygenated compounds and higher alcohols. These ideas do not contradict the findings of Hall, Kokes, and Emmett (*13*), who showed that their data could be explained by passage through *–CHOH or $*CH_2$. However, these intermediates need be present on the surface only in small coverage; most of the surface is covered by *–C and *–H. The insensitivity of the product chain length to conversion is evidence that all the reactions after hydrogenation of X are rapid and coverage by subsequent intermediates is low.

SUMMARY

The preceding discussion is summarized by the sequence of steps given below. As already mentioned, the surface at steady state is iron covered mostly by surface carbon, with small amounts of CO, H, and O, plus chain fragments. The bulk of the steady-state catalyst, for 10% CO/H_2 feed and low conversion, is Fe_2C.

For methanation:

$$H_2 \rightarrow 2*\text{–}H$$
$$CO \rightarrow *\text{–}CO$$
$$*\text{–}CO \rightarrow *\text{–}C + *\text{–}O$$
$$*\text{–}C + *\text{–}H \rightarrow *\text{–}CH$$
$$*\text{–}CH + 3*\text{–}H \rightarrow CH_4$$
$$2*\text{–}C + Fe \rightleftarrows Fe_2C$$
$$*\text{–}O + *\text{–}CO \rightarrow CO_2$$
$$*\text{–}O + 2*\text{–}H \rightleftarrows *\text{–}H_2O$$
$$*\text{–}H_2O \rightleftarrows H_2O$$

For chain growth (*22*):

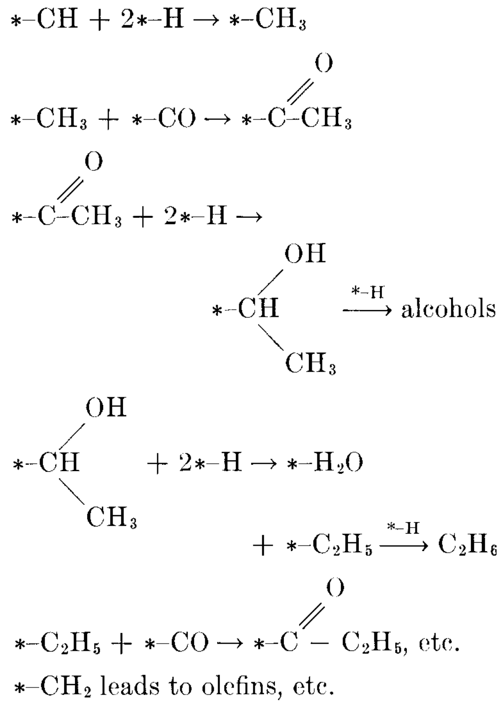

$$*\text{–}CH + 2*\text{–}H \rightarrow *\text{–}CH_3$$
$$*\text{–}CH_3 + *\text{–}CO \rightarrow *\text{–}\overset{O}{\overset{/\!/}{C}}\text{–}CH_3$$
$$*\text{–}\overset{O}{\overset{/\!/}{C}}\text{–}CH_3 + 2*\text{–}H \rightarrow *\text{–}\underset{\diagdown CH_3}{\overset{\diagup OH}{CH}} \xrightarrow{*\text{–}H} \text{alcohols}$$
$$*\text{–}\underset{\diagdown CH_3}{\overset{\diagup OH}{CH}} + 2*\text{–}H \rightarrow *\text{–}H_2O + *\text{–}C_2H_5 \xrightarrow{*\text{–}H} C_2H_6$$
$$*\text{–}C_2H_5 + *\text{–}CO \rightarrow *\text{–}\overset{O}{\overset{/\!/}{C}} - C_2H_5, \text{ etc.}$$

$*\text{–}CH_2$ leads to olefins, etc.

REFERENCES

1. Vannice, M. A., *J. Catal.* **37**, 462 (1975); Vannice, M. A., *J. Catal.* **37**, 449 (1975); Ollis, D. F., and Vannice, M. A., *J. Catal.* **38**, 514 (1975); Vannice, M. A., *J. Catal.* **40**, 129 (1075).

2. Dalla Betta, R. A., Piken, A. G., and Shelef, M., *J. Catal.* **35**, 54 (1974).

3. Kobayashi, H., and Kobayashi, M., *Catal. Rev.-Sci. Eng.* **10**, 139 (1974).

4. Bennett, C. O., *Catal. Rev.-Sci. Eng.* **13**, 121 (1976).

5. Fischer, F., and Tropsch, H., *Brennst. Chem.* **7**, 97 (1926).

6. Craxford, S. R., and Rideal, E. K., *J. Chem. Soc.* 1604 (1939).

7. Pichler, H., *Chem. Techn.* **18**, 392 (1966).

8. Eidus, Ya. T., and Zelinskii, N. D., *Izv. Akad. Nauk SSSR Otd. Khim. Nauk* 190 (1942).

9. Wentrick, P. R., Wood, B. J., and Wise, H., *J. Catal.* **43**, 363 (1976).

10. Araki, M., and Ponec, V., *J. Catal.* **44**, 439 (1976).

11. Storch, H. H., Golumbic, N., and Anderson, R. B., "The Fischer–Tropsch and Related Synthesis." John Wiley and Sons, New York, 1951.

12. Kummer, J. T., and Emmett, P. H., *J. Amer. Chem. Soc.* **75**, 5177 (1953).

13. Hall, W. K., Kokes, R. J., and Emmett, P. H., *J. Amer. Chem. Soc.* **82**, 1027 (1960).
14. Borghard, W. G., private communication, 1977.
15. Solbakken, V., Solbakken, Å., and Emmett, P. H., *J. Catal.* **15**, 90 (1969).
16. Pommier, B., and Reymond, J.-P., private communication, 1978.
17. Anderson, R. B., Hofer, L. J. E., Cohn, M. E., and Seligman, B., *J. Amer. Chem. Soc.* **73**, 944 (1950).
18. Tøttrup, P. B., *J. Catal.* **42**, 29 (1976).
19. Bousquet, J. L., Gravelle, P. C., and Teichner, S. J., *Bull. Soc. Chim. Fr.* 3693 (1972).
20. Dry, M. E., *Ind. Eng. Chem. Prod. Res. Dev.* **15**, 282 (1976).
21. Podgurski, H. H., Kummer, J. T., DeWitt, T. W., and Emmett, P. H., *J. Amer. Chem. Soc.* **72**, 5382 (1950).
22. van Barneveld, W. A. A., and Ponec, V., *J. Catal.*, **15**, 426 (1978).